1-1-2019

Variations In the Abundance and Distribution of Aggregates In the Ross Sea, Antarctica

Vernon L. Asper
University of Southern Mississippi

Walker O. Smith
Virginia Institute of Marine Science

ELEMENTA
Science of the Anthropocene

Asper, VL and Smith, WO. 2019. Variations in the abundance and distribution of aggregates in the Ross Sea, Antarctica. *Elem Sci Anth,* 7: 23. DOI: https://doi.org/10.1525/elementa.355

RESEARCH ARTICLE

Variations in the abundance and distribution of aggregates in the Ross Sea, Antarctica

Vernon L. Asper* and Walker O. Smith†,‡

The vertical distribution and temporal changes in aggregate abundance and sizes were measured in the Ross Sea, Antarctica between 2002 and 2005 to acquire a more complete understanding of the mechanisms and rates of carbon export from the euphotic layer. Aggregate abundance was determined by photographic techniques, and water column parameters (temperature, salinity, fluorescence, transmissometry) were assessed from CTD profiles. During the first three years the numbers of aggregates increased seasonally, being much more abundant within the upper 200 m in late summer than in early summer from 50 to 100 m (12.5 L^{-1} in early summer vs. 42.9 L^{-1} in late summer). In Year 4 aggregate numbers were substantially greater than in other years, and average aggregate abundance was maximal in early rather than late summer (177 vs. 84.5 L^{-1}), which we attributed to the maximum biomass and aggregate formation being reached earlier than in other years. The contribution of aggregate particulate organic carbon to the total particulate carbon pool was estimated to be 20%. Ghost colonies, collapsed colonies of the haptophyte *Phaeocystis antarctica*, were observed during late summer in Year 4, with maximum numbers in the upper 100 m of ca. 40 L^{-1}. Aggregate abundance, particulate organic carbon and ghost colonies all decreased exponentially with depth, and the rate of ghost colony disappearance suggested that their contribution to sedimentary input was small at the time of sampling. Bottom nepheloid layers were commonly observed in late summer in both transmissometer and aggregate data. Late summer nepheloid layers had fluorescent material within them, suggesting that the particles were likely generated during the same growing season. Longer studies encompassing the entire production season would be useful in further elucidating the role of these aggregates in the carbon cycle of these regions.

Keywords: Ross Sea; Antarctica; Phaeocystis; Marine snow; Carbon export

1. Introduction

The Ross Sea is the largest area of elevated pigment concentrations and primary productivity in the Antarctic, and is characterized by intense phytoplankton blooms during austral spring and summer (Smith et al., 2014). These blooms are critical contributors to biogeochemical cycles and food web dynamics of the region (Arrigo et al., 2008; Smith et al., 2014). Vertical flux rates have been estimated using sediment traps and elemental budgets (Dunbar et al., 1998; Sweeney et al., 2000a, b; Asper and Smith, 2001; Smith et al., 2011b) and appear to be substantial. Although the Ross Sea has been the focus of numerous investigations (Smith and Nelson, 1985; Arrigo et al., 1999; Smith et al., 2000, 2013), questions remain about the fate of surface production, the mechanisms of transformation of the organic matter generated within these blooms, and the rates of input to the sediments of the continental shelf.

In most years the colonial haptophyte *Phaeocystis antarctica* blooms in austral spring, followed by a diatom growth and accumulation in summer (Arrigo et al., 1999; Smith et al., 2000, 2011a). Both blooms result in extensive concentrations of biogenic material in the upper water column (e.g., biogenic silica and particulate organic carbon concentrations >60 and 85 μmol L^{-1}, respectively; Smith and Nelson, 1985; Smith et al., 1996). The blooms of *P. antarctica* are also notable for the significant amounts of organic matter that are partitioned into its mucoid envelope (Mathot et al., 2000), and these blooms reduce the dissolved iron to limiting concentrations (less than 0.1 nM) by mid-November (Sedwick et al., 2011). Growth of diatoms in austral summer is apparently supported by recycled iron, new inputs from the atmosphere, unique acclimations to low iron concentrations, or an exceptional ability to use low bioavailable iron (Smith and Kaufman, 2018).

As a bloom progresses, biomass accumulates in the euphotic zone, but the concentration of chlorophyll *a* (hereafter chlorophyll) decreases rapidly in late December

* Department of Marine Science, University of Southern Mississippi, Stennis Space Center, Mississippi, US

† Virginia Institute of Marine Science, William and Mary, Gloucester Pt., Virginia, US

‡ School of Oceanography, Shanghai Jiao Tong University, Shanghai, CN

Corresponding author: Vernon L. Asper (Vernon.Asper@gmail.com)

and early January, despite the favorable irradiance and macronutrient regime (Asper and Smith, 1999; Smith et al., 2000, 2011a; Jones and Smith, 2017). Although export via fecal pellets can be substantial over short time scales (Gowing et al., 2001; Smith et al., 2011b), average losses on an annual basis from the surface layer resulting from grazing by meso- or microzooplankton are small over much of the southern Ross Sea (Caron et al., 2000; Tagliabue and Arrigo, 2003; Mosby and Smith, 2015).

Most export of particulate matter has been suggested to occur via aggregate formation and rapid vertical flux of large particles (Asper and Smith, 1999; Gardner et al., 2000; Asper and Smith, 2003, Jackson, 1990; Lam and Bishop, 2007; Guidi et al., 2009; Burd and Jackson, 2009). The processes and factors that control the formation and degradation of aggregates have been investigated experimentally (Kiørboe and Hansen, 1993; Passow et al., 1994; Iversen and Ploug, 2013) as well as observed in situ. Aggregate production is thought to be a function of particle concentration, particle stickiness, interactions with transparent exopolymer particles (Passow et al., 1994), and the number of collisions between particles. Aggregate formation is also influenced by the composition of surface phytoplankton (Smith and Asper, 2001; Guidi et al., 2009; Giering et al., 2016; Bach et al., 2016).

While these processes have been shown to be active in the Ross Sea, sinking of *Phaeocystis antarctica* colonies represents an additional potential export mechanism (DiTullio et al., 2000). *Phaeocystis* is a widely distributed species in the Southern Ocean, and often forms dense blooms (Lancelot et al., 1998; Schoemann et al., 2005; Smith et al., 2014), especially in the Ross Sea. It has a multiphasic life cycle that includes solitary, flagellated cells of ca. 5 μm in length, as well as colonies of non-flagellated cells of similar size embedded in mucopolysaccharide envelopes. These colonies can reach 2 mm in diameter. During active growth, colonies of *P. antarctica* do not sink measurably; however, as their growth becomes limited by an environmental factor (such as irradiance or trace metal concentration), the colonies sink rapidly (Becqvort and Smith, 2000; Smith et al., 2011a; Jones and Smith, 2017), and their abundance in the euphotic zone is quickly reduced. Wassmann et al. (1990) observed colonial material that was largely devoid of cells but still recognizable as intact envelopes, and called these "ghost colonies". They speculated that the individual cells were liberated from the envelope upon growth limitation and as the colonies sank from the euphotic zone. Ghost colonies are exceptionally difficult to collect using routine water sampling procedures due to their fragile nature, and therefore their role in the life cycle of *P. antarctica* is largely unknown. Similarly, their vertical distribution and role in the vertical flux of particles are also unknown. Smith et al. (2017) estimated the abundance of distribution of ghost colonies in the Ross Sea using a Video Plankton Recorder, but those data did not provide insights into the role they play in vertical flux.

Ascertaining the role of aggregates in particle and carbon dynamics is notoriously difficult because of the fragile nature of the aggregates and their tendency to adhere to the surfaces of any sampling gear. This difficulty results in the need for alternative techniques to quantify their concentrations; e.g., collection by divers (Alldredge, 1998), high resolution in situ photography (Honjo et al., 1984), and optical procedures (Bishop et al., 2004; Smith et al., 2017). These techniques have been applied in a number of systems, but they are only semi-quantitative. As a result a quantitative understanding of the role of aggregates in oceanic biogeochemical cycles remains incomplete (Riebesell, 1993). This paper reports the results of a four-year investigation of the abundances, sizes and distributions of aggregates in the southern Ross Sea (Antarctica) using an imaging technique, and their temporal patterns and relationship to environmental factors.

2. Methods

2.1. Marine snow camera

As a part of the Interannual Variability in the Ross Sea (IVARS) program (Smith et al., 2011a, b), a marine snow imaging system was deployed at 15 stations in the southern Ross Sea (**Figure 1** and **Table 1**). Most collections were conducted at two locations (called *Callinectes* and *Xiphius*) roughly 160 km apart, where moorings were deployed during the ice-free periods (Smith et al., 2011a). Profiles of images were collected from whichever ship was used (*N.B. Palmer*, *USCG Polar Star* or *Polar Sea*). The dates of sampling were determined by the ship's schedule, so the earliest profiles were acquired in late December and the latest were acquired in early February. We refer to these as austral "early summer" and "late summer", with the realization that these logistical constraints limited our coverage of the progression of the phytoplankton bloom. Cruises took place during early and late summer in 2001, 2002 (early summer only), 2003–2004, and 2004–2005; no late summer cruise was conducted in 2002 as no ship was available.

The imaging system is based on the one developed by Honjo et al. (1984). It consisted of a collimated strobe system and either a 35-mm film camera (Lobsiger Deepslope 6000; Years 1–3) or a digital camera (Insite Pacific Scorpio; Year 4) mounted on an aluminum frame (**Figure 2**). The light is collimated using a combination of a rectangular reflector that is parabolic in cross section as well as a series of baffles that absorb any light that is not within the defined column. The system was lowered at a rate of 10 m min^{-1} through the water column, acquiring six images min^{-1} resulting in a depth interval of ca. 1.7 m. Illumination was provided by a pair of strobe lights (Deep Sea Power and Light) positioned to produce an 8.4-cm deep beam of uniform, collimated light 66 or 79 cm from the camera lens (**Figure 2**). Aggregates larger than 0.5 mm within this volume (3–15 L, depending on camera, lens, zoom setting, and resultant geometry) are quantified from images taken by a camera that is mounted perpendicular to the long axis of the light beam. Ambient light illuminates particles in front of and behind this light beam and invalidates the calculation of illuminated volume. Thus, profiles were obtained near local midnight

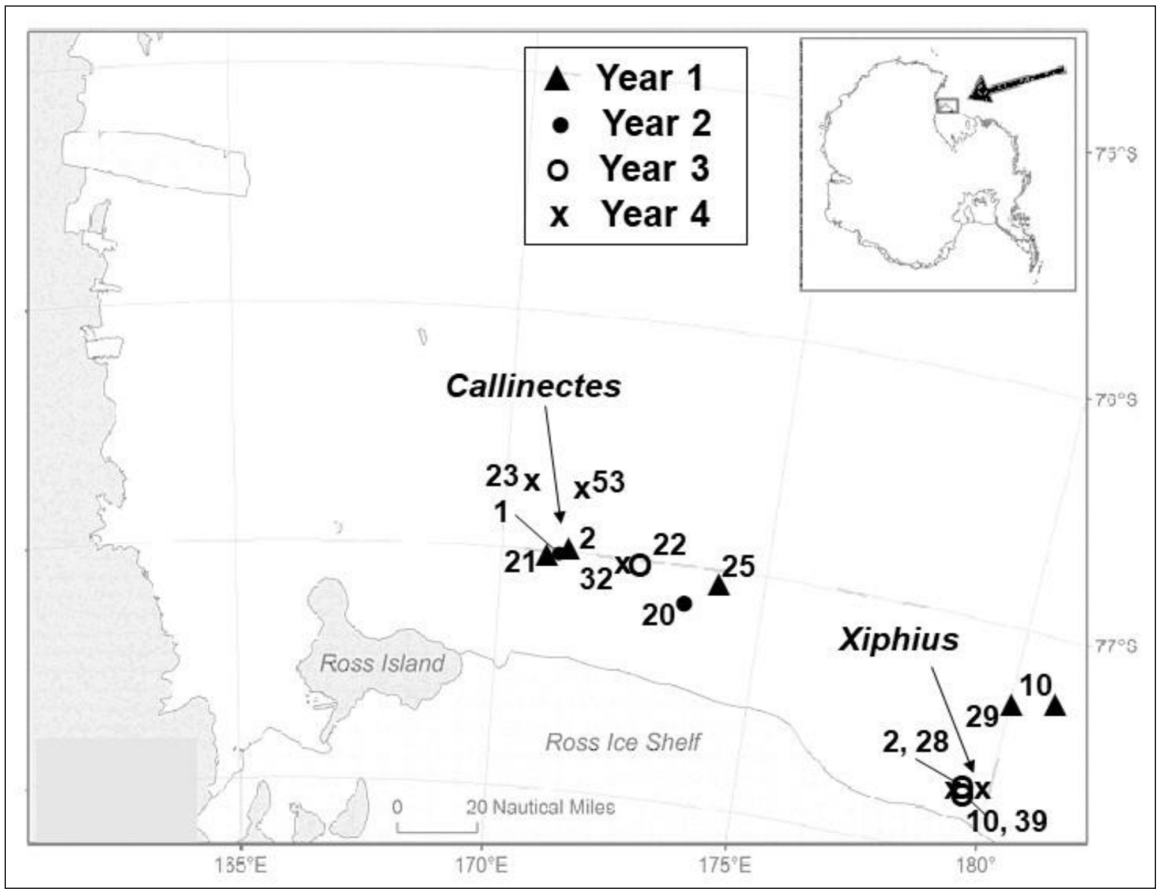

Figure 1: Location map. Map showing the location of aggregate profiling stations by their numbered designations in the southern Ross Sea. *Callinectes* and *Xiphius* are the named locations of moorings where most observations were collected. DOI: https://doi.org/10.1525/elementa.355.f1

Table 1: Location and dates of aggregate profile collection and imaging system used. DOI: https://doi.org/10.1525/elementa.355.t1

Cruise, station no.[a]	Latitude (°S)	Longitude (°)	Date (mo/day/year)	Photographic method
Year 1, 2 (C)[a]	76.987	171.935 E	12/20/2001	Film
Year 1, 10 (X)[a]	77.553	177.977 W	12/22/2001	Film
Year 1, 21 (C)	77.008	171.826 E	2/4/2002	Film
Year 1, 25	77.103	174.408 E	2/5/2002	Film
Year 1, 29 (X)	77.460	178.771 W	2/6/2002	Film
Year 2, 1 (C)	76.967	171.950 E	12/25/2002	Film
Year 2, 20	77.283	173.839 E	12/27/2002	Film
Year 3, 2 (X)	77.668	180.000	12/29/2003	Film
Year 3, 22 (C)	77.000	172.800 E	2/6/2004	Film
Year 3, 28 (X)	77.668	180.000	2/5/2004	Film
Year 4, 10 (X)	77.668	180.000	12/23/2004	Digital
Year 4, 23 (C)	76.4095	171.067 E	12/24/2004	Digital
Year 4, 32 (C)	77.000	172.800 E	1/29/2005	Digital
Year 4, 39 (X)	77.668	180.000	1/30/2005	Digital
Year 4, 53 (C)	76.410	171.784 E	2/1/2005	Digital

[a] C = near the mooring location *Callinectes*; X = near the mooring location *Xiphius.*

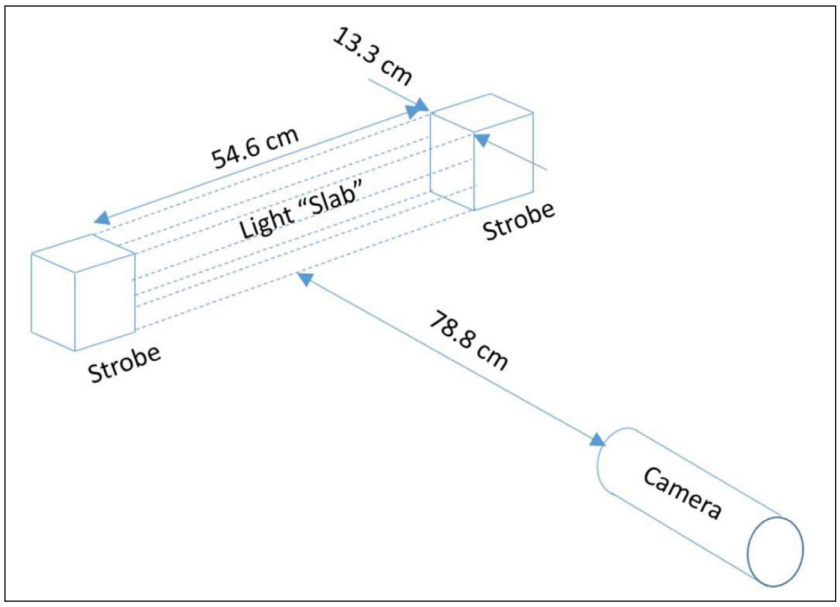

Figure 2: Configuration of the aggregate imaging system. Schematic showing the arrangement of the aggregate imaging system used to visualize aggregates in the Ross Sea. DOI: https://doi.org/10.1525/elementa.355.f2

whenever possible (although 24-h photoperiods occurred throughout all cruises) to minimize this interference; images with the frame visible, due to ambient light, were discarded. The depth of first aggregate counts ranged from 30 to 88 m (a function of water clarity and solar angle); however, because the numbers of aggregate observations in the upper 50 m were limited due to excess light, we have removed all data from this depth range. A Sea-Bird SeaCat CTD and 25-cm SeaTech transmissometer mounted on the camera frame provided depth measurements as well as continuous measurements of temperature, salinity and optical transmission, although these data are not presented here. CTD casts were taken immediately before camera casts as well, using the ship's calibrated CTD-rosette system (SeaBird 911+) with an in situ fluorometer, transmissometer and PAR sensor mounted on the rosette.

All film (Tmax 400) and images were returned to the laboratory for processing except for short sections viewed at sea to assess camera operation. The films were developed and digitized to JPG format either in-house, using a Nikon camera and macro lens (3767 × 2368), or commercially (3544 × 2341). They were then analyzed using Image Pro Plus®, with a final resolution of the digitized images (2048 × 1536 pixels) of 4.2 pixels mm^{-1}. Digital images were analyzed directly with a final resolution of 4.2 pixels mm^{-1}. To insure that the same portion of each image was analyzed, an area of interest was created within the region of maximum illumination and then positioned to the same location within each image before particles were counted. Objects that were clearly not aggregates, such as large zooplankton, were excluded from the counts, but small zooplankton, phytoplankton colonies, fecal material, and other objects were likely included. Aggregate measurements included length, width, maximum diameter, perimeter, aspect ratio, and area, but all lengths reported are those of the longest dimension of each aggregate, which was usually close to the vertical axis. For the most part *P. antarctica* colonies could not be resolved in our system, but ghost colonies were observable due to their increased opacity.

Although every effort possible was expended to ensure accuracy, imaging techniques are inherently subjective and variable. Challenges include variations in light intensity across the light beam, potential variations in the output of the strobe, the effect of small particles on the attenuation of the light, interference from particles between the light beam and the camera, and, in the case of film images, variations in the chemical processing of the films. Digital image analyses are also vulnerable to the user interaction and especially to the threshold setting used. A setting that is too low will result in artificially high particle counts; settings that are too high will exclude valid particles. To minimize this error, tests were performed wherein multiple operators were asked to assign a threshold level to determine the potential error caused by user variations. The result of these tests showed that these threshold variations mostly affected the very small (1 or 2 pixels) particles. Because we eliminated particles smaller than 0.5 mm, we are confident that these variations had no important impact on the accuracy of the results.

A further complication was added by the switch from film to digital imagery in Year 4, even though the same strobe system was used. Because only one of these strobe light systems exists, deploying both the film and digital cameras simultaneously was not possible, and no laboratory comparisons are available. However, comparisons of deep water images (where variability is reduced) from the two cameras suggest that the digital system may be more sensitive. These comparisons suggest that the difference between the two did not result in higher numbers of identifiable aggregates than did the film system. Changes with depth and season are consistent and independent of the technique.

2.2. Carbon calculations

Although the composition of aggregates is variable in space and time, estimating their carbon content using results from diver-collected individual aggregate samples is useful (Alldredge, 1998). As with any oceanic ecosystem, the aggregates in the Ross Sea likely have a different composition than those in the Alldredge study, which were mostly from a coastal California environment, but application of the reported regressions provides a sense of the potential carbon content and allows for comparison to other measurements. We applied the Alldredge regressions to the volumes of the aggregates, which were calculated using the average diameter of each aggregate and assuming a spherical shape. We refer to the estimated aggregate POC as APOC to distinguish it from total POC (particulate organic carbon) estimated from transmissometry.

Data from the rosette transmissometer and POC data from bottle samples were used to generate a regression and then to calculate the contribution of small particles to the POC using the equation:

$$\mathrm{POC}\ \left(\mu\mathrm{mol\ L^{-1}}\right) = -2.14c_p - 2.14\ \left(R^2 = 0.91\right)$$

where c_p is the beam attenuation coefficient due to particles, which in turn is determined from the percentage transmission (Gardner et al., 1995) with attenuation due to water removed. Similarly, fluorescence data (Fl) were used to calculate the chlorophyll (Chl) content using the equation:

$$\mathrm{Chl}\ \left(\mu\mathrm{g\ L^{-1}}\right) = 1.56\mathrm{Fl} - 0.050\ \left(R^2 = 0.81\right)$$

which was derived from a least squares analysis of discrete chlorophyll determinations and fluorescence values at the same depths. Additional information concerning the physical, chemical and biological conditions at the time of the imaging casts can be found in Smith et al. (2011a, b). Mixed layer depth was defined as the depth where a change of 0.01 kg m^{-3} in sigma-T from the stable surface layer occurred (Thompson and Fine, 2003; Smith et al., 2013). Total depth at most stations was ca. 650 m. All statistical analyses were completed using SigmaPlot 12.3.

3. Results

3.1. General hydrographic conditions

Ice concentrations in the Ross Sea change rapidly during late austral spring and are variable from year to year. In a typical year, the polynya expands largely in the south-north direction, and some residual ice remains in the western portions of the southern Ross Sea (Smith et al., 2011a). Consequently, early summer stations that were occupied in the western areas had reduced (<20%) ice cover, while the eastern stations were completely ice-free. By the time of the late summer cruise, nearly all ice had disappeared from both sampling areas. The early summer cruises were always characterized by large surface chlorophyll and particulate organic carbon concentrations and relatively shallow mixed layers (**Table 2**; Smith et al., 2011a); by February the biomass levels had decreased in most years, and mixed layers had begun to deepen (**Table 2**). Early summer phytoplankton in the southern Ross Sea were dominated by the haptophyte *Phaeocystis antarctica*, but late summer assemblages were dominated by diatoms (Smith et al., 2011a). However, variations among years were substantial (Smith et al., 2006). For example, in Year 2 ice concentrations were greatly elevated due to the presence of a massive iceberg (C-19) that had grounded in the northern Ross Sea, which in turn reduced the northerly advection and reduction of pack ice in the south, which in turn reduced *in situ* irradiance, greatly reducing phytoplankton growth and biomass accumulation. In Year 3 diatoms appeared to be more common during both seasons, and a secondary bloom was observed in late summer that was of similar magnitude as the spring bloom, whereas in Year 4 no secondary bloom was observed (Smith et al., 2006, 2011a). Macronutrient concentrations remained elevated during all cruises (Smith et al., 2011a) and above levels considered to be limiting.

3.2. Vertical profiles

3.2.1. Changes with depth and season: Vertical distributions of aggregates and their properties

In all casts aggregates were most abundant in the upper 100 m, and aggregate numbers declined rapidly below that (**Figure 3**). Mean abundances by depth interval in Year 4 were greater than means of Years 1–3 combined (**Figure 3**). At 400 m, a depth where aggregate abundance approached its vertical minimum, the difference between Years 1–3 and Year 4 was ca. 4-fold. The vertical patterns observed in all years, however, were the same. Late summer aggregative abundance at the water column minimum was reduced to concentrations that were ca. 10% of those above 100 m, but they were slightly elevated within 50 m of the bottom, suggesting that the increases near the bottom resulted from the resuspension of aggregates that had sunk from the surface layer generated during the productive spring and early summer.

In the early summer of Year 4, aggregate abundance was substantially elevated (**Figure 3**). The maximum abundance observed at all stations occurred in early summer in Year 4 (287 L^{-1}), compared to a maximum during Years 1–3 (both seasons) of 129 L^{-1}. We interpret these findings as indication that the processes that generate aggregates were more temporally advanced during early summer of Year 4, resulting in a greater production and abundance earlier than in other years. Continuous fluorescence data support the contention that the early summer bloom maximum in Year 4 was earlier (Smith et al., 2011a), and, as aggregate abundance is linked to surface particle production, elevated abundances in Year 4 likely resulted from the temporal dynamics of the bloom. Mean mixed layer POC concentrations were greater in Year 4 than in the early summer of Years 1–3 (**Table 2**), consistent with the suggestion that the bloom was in a more advanced stage than in other years (Smith et al., 2011a).

The average early and late summer aggregate concentrations (Years 1–3) were 3.30 and 43.9, 2.23 and 24.8, and

Table 2: Summary of oceanographic conditions encountered during the image system casts. DOI: https://doi.org/10.1525/elementa.355.t2

Cruise/station no.[a]	Date (mo/day/year)	Z_{mix}[b] (m)	Z_{mix} chlorophyll (μg L^{-1})	Z_{mix} POC (μmol L^{-1})	Dominant phytoplankton functional group
Year 1, 2 (C)[a]	12/20/2001	25	7.56	5.26	*Phaeocystis antarctica*
Year 1, 10 (X)[a]	12/22/2001	29	6.36	42.9	*P. antarctica*
Year 1, 21 (C)	2/4/2002	12	4.95	25.3	Diatoms
Year 1, 25	2/5/2002	28	7.82	17.7	*P. antarctica*, diatoms
Year 1, 29 (X)	2/6/2002	26	2.73	17.6	Diatoms
Year 2, 1 (C)	12/25/2002	21[c]	6.75	ND[d]	*P. antarctica*, diatoms
Year 2, 20	12/27/2002	50[c]	0.30	ND[d]	Diatoms, *P. antarctica*
Year 3, 2 (X)	12/29/2003	41	9.39	41.1	Diatoms, *P. antarctica*
Year 3, 22 (C)	2/6/2004	40	7.95	34.8	Diatoms
Year 3, 28 (X)	2/5/2004	23	14.2	29.9	Diatoms
Year 4, 10 (X)	12/23/2004	21	10.6	56.3	*P. antarctica*
Year 4, 23 (C)	12/24/2004	27	7.35	56.0	Diatoms
Year 4, 32 (C)	1/29/2005	36	0.47	12.6	*P. antarctica*, diatoms
Year 4, 39 (X)	1/30/2005	45	0.39	13.1	Diatoms
Year 4, 53 (C)	2/1/2005	31	0.66	10.7	Diatoms

[a] C = near the mooring location *Callinectes*; X = near the mooring location *Xiphius*.
[b] Depth of mixed layer.
[c] CTD data unavailable due to CTD loss; mixed layer depths estimated from vertical distribution of nutrient concentrations.
[d] No data.

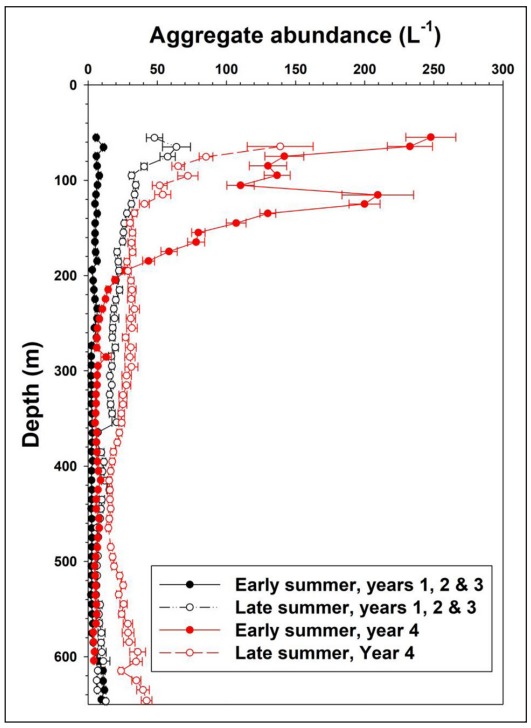

Figure 3: Comparative depth profiles of aggregate abundances by year. Mean vertical distribution of aggregate abundance (10-m bins) in the southern Ross Sea during early and late summer for Years 1–3 and Year 4. Bars represent standard errors; n = 2–5. DOI: https://doi.org/10.1525/elementa.355.f3

2.35 and 25.2 L^{-1} in the depth intervals of 50–100, 100–200, and 200–300 m, respectively (**Table 3**). Vertically integrated aggregate numbers were over five times greater in late summer (11,310 vs. 2,084 m^{-2}; late December vs. early February) in Years 1–3, suggesting that the process of aggregate formation was temporally decoupled from surface biomass levels, which are maximal in mid- to late December (Smith et al., 2011a, 2014; Jones and Smith, 2017). Year 4, however, exhibited a decrease in aggregate numbers in late summer relative to early summer (15,960 vs. 21,720 m^{-2}; **Table 3**), but we believe that this decrease was due to the temporal progression of the bloom, with aggregate formation being maximal earlier in the season in that year.

Aggregate abundance was also elevated within a bottom nepheloid layer in ca. half of the late summer profiles (**Figure 3**), suggesting a frequent resuspension of particles that were relatively buoyant. These nepheloid layers showed little enhancement in early summer profiles of aggregate abundance, pigments or organic matter, but late summer nepheloid layers included some pigmented particles as well as particulate organic carbon (**Figure 4**). The presence of pigmented material in these layers suggests that the resuspended organics were relatively "new" and probably originated within the same year.

3.2.2. Changes in size of aggregates

Aggregate size in both seasons and at all depths was dominated by the smaller size (0.5–1.0 mm; **Figure 5**), and the contribution of each size class was reasonably constant

Table 3: Abundance of aggregates by year, season, depth, and the first three years combined. DOI: https://doi.org/10.1525/elementa.355.t3

Year	Season	Depth interval (m)	Aggregate abundance[a] (no. L^{-1})	N value (no. of images)
1	Early summer	50–100	3.30 ± 1.28	87
		100–200	2.23 ± 1.08	186
		200–300	2.35 ± 0.87	240
	Late summer	50–100	43.9 ± 17.8	104
		100–200	24.8 ± 12.5	183
		200–300	25.2 ± 7.80	127
2	Early summer	50–100	10.3 ± 9.08	159
		100–200	7.29 ± 7.60	211
		200–300	7.51 ± 9.55	234
3	Early summer	50–100	11.3 ± 3.00	35
		100–200	5.94 ± 2.72	72
		200–300	1.72 ± 0.56	70
	Late summer	50–100	67.0 ± 9.97	59
		100–200	111 ± 19.5	107
		200–300	24.5 ± 12.2	42
4	Early summer	50–100	177 ± 72.6	90
		100–200	103 ± 66.6	185
		200–300	10.3 ± 5.95	90
		50–640[b]	21,720	1
	Late summer	50–100	84.5 ± 42.7	51
		100–200	37.1 ± 18.8	183
		200–300	29.0 ± 14.7	185
		50–640[b]	15,660	2
Years 1–3	Early summer	50–100	12.5 ± 13.2	307
		100–200	12.2 ± 13.5	593
		200–300	9.45 ± 10.9	659
		50–640[b]	2,080	2
	Late summer	50–100	42.9 ± 27.3	107
		100–200	28.1 ± 18.4	207
		200–300	15.5 ± 5.20	143
		50–640[b]	11,310	2

[a] Mean ± standard deviation.
[b] Stations where data were collected to a depth of 640 m for full water-column integration.

with depth in both early and late summer (**Table 4**). The number of aggregates decreased exponentially with depth, although there was a slight increase in the largest size class in late summer in all three depth ranges. The general exponential increase is consistent with the concept that larger aggregates sink faster and hence were less likely to be imaged than the smaller ones.

3.2.3. POC and aggregate carbon

We compared the seasonal vertical distribution of aggregate abundance to that of particulate organic carbon (calculated from beam attenuation) and chlorophyll (**Figure 4a, b**). In early summer POC was maximal in the euphotic zone and upper mixed layer, and chlorophyll exhibited a secondary maximum between 60 and 80 m. Aggregates showed a similar distribution, but the secondary maximum was between 120 and 140 m. In late summer a secondary maximum was not observed, and POC and chlorophyll were maximal in the surface layer; aggregate abundances were highly correlated with POC concentrations in the pooled seasonal data (AGG [L^{-1}] = 13.9POC [μmol L^{-1}] – 22.8; n = 104; $R^2 = 0.83$; $p < 0.001$). No obvious relationship to water column vertical density distributions was observed in either season.

The contribution of aggregate particulate organic carbon (APOC) also varied with season and depth (**Table 5**). Means for early and late summer (Years 1–3) indicate that APOC was greatest in late summer (about twice that in early summer), a pattern also seen in total aggregate abundance. In Year 4 early summer APOC contribution in the entire water column was five-fold greater than in the previous three years (reflecting the increased abundance of aggregates in early summer of Year 4), while late summer APOC was only 33% greater (**Tables 4, 5**). This difference suggests that the substantial early summer APOC either sank to the benthos or was remineralized within the water column, so that late summer conditions were similar to the previous years. Early summer carbon:chlorophyll ratios in Year 4 were also elevated relative to those normally associated with the *P. antarctica* bloom (94.8 vs. ca 45; Kaufman et al., 2014; Jones and Smith, 2017; Smith and Kaufman, 2018), which implies that the bloom had progressed more rapidly and transitioned from *Phaeocystis* to diatoms earlier than in the previous years.

3.3. Phaeocystis ghost colonies

In addition to the aggregates, we identified particles in Year 4 as *Phaeocystis* colonies that appeared to be collapsed and devoid of cells (**Figures 6, 7**). Based on the description by Wassmann et al. (1983) and Smith et al. (2017), we categorized these as "ghost colonies". Ghost colonies were not observed during Years 1–3, possibly due to the reduced sensitivity of the photographic procedures, but their appearance is also influenced by the presence of colonial *P. antarctica* in the euphotic zone, which also varied among years. Ghost colonies have been observed via photography in other studies (V Asper, unpubl.), suggesting that the major difference among years was controlled by phytoplankton composition. The abundance of ghost colonies in Year 4 increased from nearly zero (**Figure 8**) in the early summer to more than 40 L^{-1} in the late austral summer. Mean ghost colony abundance in late summer (3.83 mL^{-1}) was more than five-fold greater than in early summer (0.74 mL^{-1}) and, in the upper 150 m, over an order of magnitude greater than in early summer. Ghost colonies were observed in deeper waters (within 50 m of the bottom), but only rarely. Ghost colony abundance (GCA) was correlated with aggregate abundance

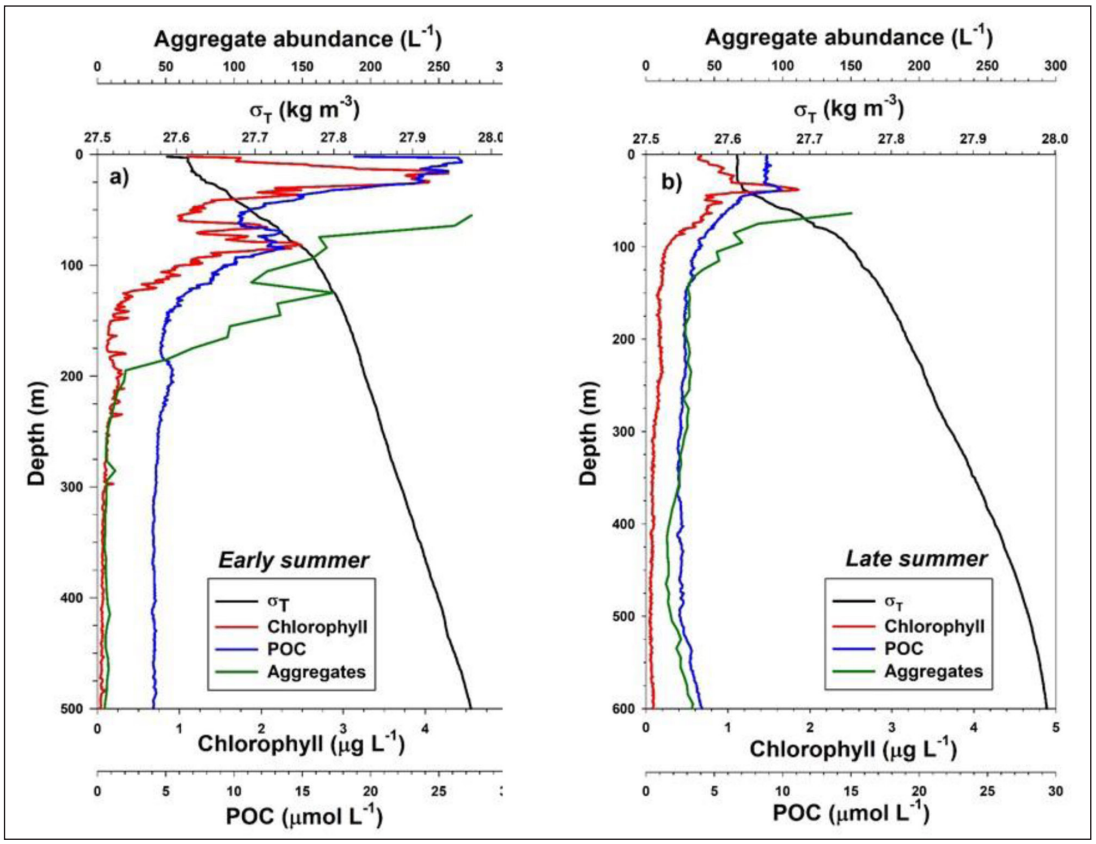

Figure 4: Comparative depth profiles of aggregate abundance and other parameters in Year 4. a) Year 4 vertical distribution of mean aggregate abundance, water column density (σ_T), chlorophyll concentration (μg L^{-1}) and particulate organic carbon concentration (POC; μmol L^{-1}) in a) early summer (n = 3) and **b)** late summer (n = 2). Chlorophyll and POC were derived from CTD profiles of fluorescence and optical transmission. Scales are the same in both panels to facilitate comparison. DOI: https://doi.org/10.1525/elementa.355.f4

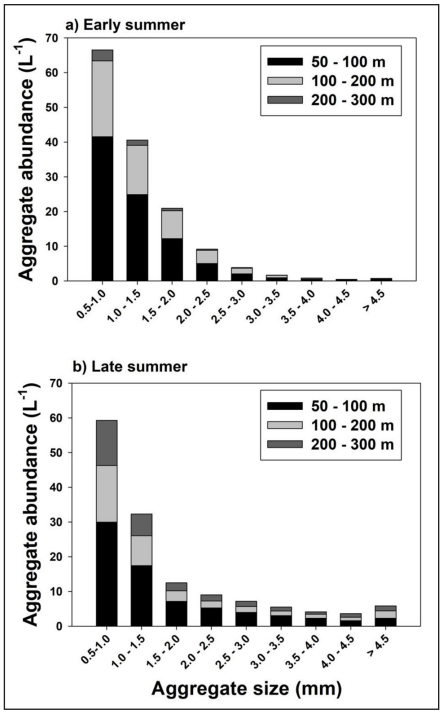

Figure 5: Aggregate sizes by depth interval. Size distribution of aggregates (mean of all years) for **a)** early summer and **b)** late summer. Sizes differentiated by maximum axis length. DOI: https://doi.org/10.1525/elementa.355.f5

(AA) in both seasons, but with substantially different slopes: early summer GCA = 0.0038AA + 0.36; n = 21, $r^2 = 0.68$, $p < 0.001$ (t-test); late summer GCA = 0.27AA – 6.32, n = 33, $r^2 = 0.93$, $p < 0.001$ (t-test). Taken together, these results suggest that the process of formation of both aggregates and ghost colonies was linked to the surface particulate organic matter load, but delivery to depth had a significant temporal delay. Based on the rarity of ghost colony occurrence within the nepheloid layers, as well as their exponential disappearance within the water column, we do not believe that they are major contributors to flux to the sediments. However, rapidly sinking particles are rarely found in our images (that is, there is an inverse relationship between sinking speed and abundance, as fast-sinking particles rapidly disappear from the water column and are inadequately sampled using our technique). Hence, the role of ghost colonies in vertical flux remains uncertain.

4. Discussion

Aggregates commonly contribute to the particulate organic matter stocks in the water column of the Ross Sea, as in the rest of the ocean. Ross Sea aggregates have been suggested to form from material generated during the spring *Phaeocystis antarctica* bloom (Asper and Smith, 2001) and rapidly sink from the surface layer, and similar relationships between phytoplankton biomass and aggregates have been observed elsewhere (Lampitt et al., 1993;

Table 4: Percentage contribution of various size classes to the total abundance of aggregates as a function of depth. DOI: https://doi.org/10.1525/elementa.355.t4

Season	Aggregate size class (mm)	Percentage by depth interval[a] (m)		
		50–100	100–200	200–300
Early summer	0.5–1.0	47.2	42.9	52.0
	1.0–1.5	28.3	27.8	25.5
	1.5–2.0	13.9	15.7	12.0
	2.0–2.5	5.72	7.49	5.43
	2.5–3.0	2.36	3.22	2.27
	3.0–3.5	1.06	1.40	1.05
	3.5–4.0	0.60	0.59	0.66
	4.0–4.5	0.30	0.37	0.44
	≥4.5	0.56	0.48	0.63
Late summer	0.5–1.0	41.1	43.8	44.4
	1.0–1.5	24.0	23.1	21.3
	1.5–2.0	9.75	8.20	7.92
	2.0–2.5	7.20	5.38	6.13
	2.5–3.0	5.40	4.60	5.18
	3.0–3.5	4.16	3.51	3.98
	3.5–4.0	3.12	3.09	2.42
	4.0–4.5	2.17	2.60	3.64
	≥4.5	3.14	5.65	5.00

[a] Calculated from the integrated abundance and size classes in the depth ranges indicated.

Jackson et al., 2005; Reigstad and Wassman, 2007). Our data are consistent with that general trend; however, there are substantial variations that are regulated by specific oceanographic and biological controls. While we observed greater numbers of aggregates in late summer than during early summer (**Table 3**), this pattern was not observed in Year 4 of our study. In that year we found greater numbers of aggregates in early than late summer. Aggregate numbers in early summer of 2004 were greater than at any other period (**Figure 3**), an unusual occurrence that we attribute to the *Phaeocystis* bloom being earlier that summer, and hence a temporal shift in the aggregate production that we sampled.

Year 4 also had a greater contribution of *P. antarctica* to phytoplankton biomass than did Year 3 (which had more diatoms; Smith et al., 2011a), consistent with the suggestion of Bach et al. (2016) that both assemblage composition and overall biomass are important regulators of aggregate production. In addition, calculated early summer net community production and export were greatest in Year 4 relative to all other years (Smith et al., 2011b). Late summer production, however, was smaller relative to other years. The oceanographic conditions observed in Year 4 seem to have resulted in a larger and earlier production of phytoplankton (dominated by *P. antarctica*) and organic aggregates compared to other years.

Table 5: Estimated mean particulate organic carbon concentration contributed by aggregates by year, season, depth, and Years 1–3 combined. DOI: https://doi.org/10.1525/elementa.355.t5

Year	Season	Depth interval (m)	Aggregate POC[a] (μmol L^{-1})	N
1	Early summer	50–100	0.91 ± 0.034	87
		100–200	0.082 ± 0.038	186
		200–300	0.105 ± 0.265	239
	Late summer	50–100	0.388 ± 0.177	41
		100–200	0.310 ± 0.156	82
		200–300	0.230 ± 0.109	83
2	Early summer	50–100	0.271 ± 0.205	185
		100–200	0.237 ± 0.159	335
		200–300	0.275 ± 0.596	350
3	Early summer	50–100	0.188 ± 0.058	41
		100–200	0.175 ± 0.085	82
		200–300	0.109 ± 0.060	83
	Late summer	50–100	0.424 ± 0.187	59
		100–200	0.584 ± 0.457	109
		200–300	0.568 ± 0.236	42
4	Early summer	50–100	1.269 ± 0.449	89
		100–200	1.006 ± 0.429	185
		200–300	0.483 ± 0.286	90
		50–640[b]	2,680	1
	Late summer	50–100	0.806 ± 0.232	60
		100–200	0.477 ±0. 246	238
		200–300	0.388 ± 0.211	241
		50–640[b]	1,870	1
Years 1–3	Early summer	50–100	0.204 ± 0.176[c]	308
		100–200	0.165 ± 0.134[c]	593
		200–300	0.178 ± 0.436[c]	659
		50–640[b]	95.8[c]	1
	Late summer	50–100	0.401 ± 0.181[c]	107
		100–200	0.379 ± 0.291[c]	207
		200–300	0.316 ± 0.592[c]	143
		50–640[b]	197[c]	1

[a] Mean ± standard deviation; POC estimated by calculating the volume of each aggregate from the average dimension and assuming a spherical shape, then converting into weight assuming a density of 1.027 kg m^{-3}, porosity of 0.97, and weight per unit C ratio of 0.4.

[b] Stations where data were collected to a depth of 640 m for full water-column integration.

[c] Integral POC values in units of μmol m^{-2}.

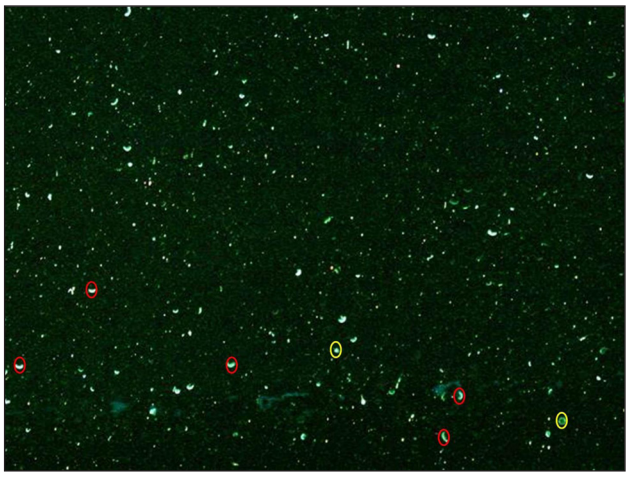

Figure 6: Typical aggregate appearance. Image of aggregates and *Phaeocystis antarctica* ghost colonies (circled in red) and intact colonies (circled in yellow) observed at Station 39 (77.67°S, 180°) at 109 m on January 30, 2005 (Year 4). DOI: https://doi.org/10.1525/elementa.355.f6

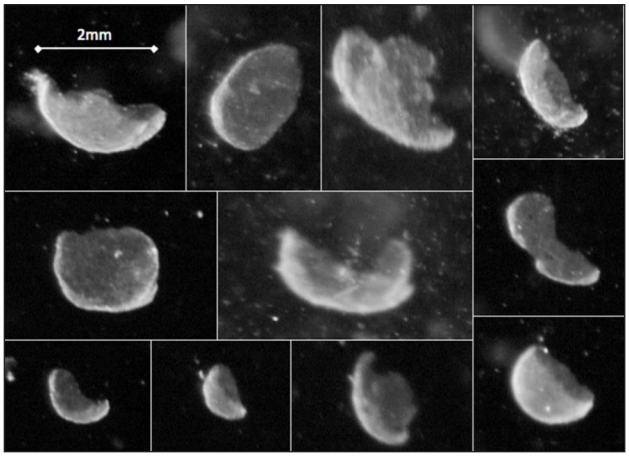

Figure 7: Views of typical ghost colonies of *Phaeocystis antarctica*. Images courtesy of D McGillicuddy (unpublished). DOI: https://doi.org/10.1525/elementa.355.f7

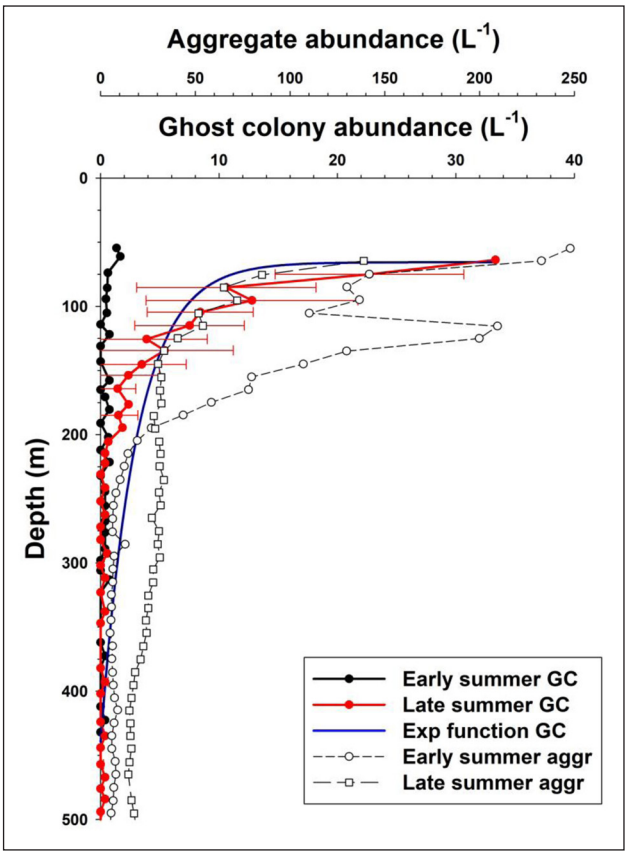

Figure 8: Abundance of ghost colonies of *Phaeocystis antarctica* in Year 4. Vertical distribution of mean abundance, with standard deviation (error bars) where available (n = 3), of *P. antarctica* ghost colonies (GC) in early (black line) and late (red line) summer in Year 4. Blue line represents the fitted exponential decay of summer ghost colonies ($GC_z = GC_0 - 374[1-e^{-0.313z}]$; $p > 0.001$). Mean aggregate abundances (aggr) in early and late summer added for comparison. DOI: https://doi.org/10.1525/elementa.355.f8

Aggregates represented a modest contribution to total standing stocks of POC. Means from the first three years suggested that aggregate POC was less than 1 µmol C L^{-1} (**Table 5**), whereas mixed layer POC ranged from 5 to 42 µmol C L^{-1} (**Table 2**). In early summer of Year 4, when aggregate numbers were greatest, water column POC was also elevated, with mixed layer POC being 56 µmol C L^{-1} (**Table 2**) and averaging 20.1 µmol C L^{-1} in the upper 50 m. Aggregate POC below 50 m was substantial; the APOC/POC ratio increased with depth, and the integrated water column contribution of aggregates was 20.8% of the total integrated POC (**Table 6**). Integrated late summer contributions were similar. These estimates suggest that aggregate POC can be an important component of the total particulate matter concentration. We recognize, however, that there are a number of assumptions inherent in this calculation. Estimating particle volume assumes a particular dimension and shape, and using Alldredge's marine snow POC regression fails to account for variations between her study area and the Ross Sea. Additionally, if aggregates sink rapidly they will not be included in our estimates of APOC. As a result, these estimates only reflect the contribution of aggregates to standing stocks of POC, and do not accurately reflect the role of aggregates in vertical flux. Despite these simplifications, such estimates are useful to begin to understand the role of aggregate POC in polar systems.

Additionally, we found a specific phase of *P. antarctica* in Year 4 — ghost colonies — that were not detected in other years. What governs the formation of ghost colonies is not at all clear, but they are likely generated upon senescence of surface layer colonies; however, there is no direct relationship between ghost colony abundance and appearance to euphotic zone *P. antarctica* colony abundance (Smith et al., 2017). Regardless, the absolute number of ghost colonies was always small relative to total numbers of other aggregates observed in the images (**Figure 8**). Hence the flux of POC to depth resulted not only from the sinking of ghost colonies, but the flux of intact colonies and colonial material that formed typical

Table 6: Seasonal mean vertical distributions in Year 4 of aggregate particulate organic carbon (APOC, generated from aggregate volume), total POC (from transmissometer data), chlorophyll (Chl; from fluorescence data), and the relative contribution of APOC to total POC. DOI: https://doi.org/10.1525/elementa.355.t6

Season	Depth interval (m)	Mean[a] Chl (μg L^{-1})	Mean[a] POC (μmol L^{-1})	Mean[a] APOC (μmol L^{-1})	POC/Chl (w/w)	APOC contribution to POC (%)
Early summer	50–100	1.55 ± 0.44 (n = 49)	11.6 ± 1.19 (n = 49)	1.27 ± 0.46 (n = 49)	89.8	11.0
	100–200	0.36 ± 0.27 (n = 99)	5.94 ± 1.43 (n = 99)	1.01 ± 0.47 (n = 99)	201	17.0
	200–300	0.15 ± 0.06 (n = 99)	4.64 ± 0.36 (n = 99)	0.48 ± 0.70 (n = 99)	362	10.3
	50–640[b]	260 ± 195 (n = 5)	3.42 ± 2.12 (n = 5)	0.71 ± 0.93 (n = 5)	157	20.8
Late summer	50–100	0.57 ± 0.19 (n = 49)	5.12 ± 0.90 (n = 49)	0.86 ± 0.34 (n = 49)	107	16.8
	100–200	0.18 ± 0.03 (n = 99)	3.12 ± 0.32 (n = 99)	0.48 ± 0.29 (n = 99)	206	15.3
	200–300	0.15 ± 0.03 (n = 99)	2.72 ± 0.14 (n = 99)	0.39 ± 0.19 (n = 99)	212	14.3
	50–640[b]	132 ± 45.1 (n = 3)	2.09 ± 0.47 (n = 3)	0.41 ± 0.47 (n = 3)	191	19.6

[a] Mean ± standard deviation.
[b] Integrated chlorophyll and POC values are in mg chl m^{-2} and mmol m^{-2}, respectively.

aggregate shapes. Another feature about ghost colonies is that they sink at all, given that they are largely organic and may have a density similar to that of seawater. Further research on these unusual features of the haptophyte life cycle may provide answers to these questions.

Smith et al. (2011b) estimated the sinking speeds of the material and sinking from the surface to 200 m by assessing the changes in time between the appearance of maximum fluorescence at 41 m and the date of appearance of the maximum organic matter concentration in time-series sediment traps with a 3-day sampling interval. These analyses suggested that the intervals between the two maxima ranged from 3 to 27 days, corresponding to a sinking speed between 6 and 53 m d^{-1}. Such rates are similar to those calculated from the time-series of POC in the southern Ross Sea (ca. 3 m d^{-1} for fluxes of chlorophyll — assumed to be intact *P. antarctica* colonies — when vertical decreases were greatest; Jones and Smith, 2017). Asper and Smith (2003) used a camera-equipped sediment trap technique and found that aggregate sinking rates ranged from 0 to 200 m d^{-1}, but only a small number of aggregates had extremely high sinking rates. As aggregates are heterogeneous both in composition, size and flux rates, generalizing about their role in carbon fluxes is difficult without a concurrent assessment of the flux rates of a large number of individual aggregates.

In other areas of the ocean, fecal pellets contribute substantially to vertical flux, and can be the quantitatively dominant form of sinking particles (Wassmann et al., 2000; Ebersbach and Trull, 2008; Cavagna et al., 2013). This biologically mediated flux is dependent on the type of grazer, the size of fecal pellets, and the rates of microbial and grazer disruption of the pellets (Giering et al., 2016). Conversely, phytodetritus and aggregates can dominate vertical fluxes at other times and locations (Alldredge and Gotschalk, 1989; Turner, 2002; De La Rocha and Passow, 2007; Burd and Jackson, 2009). Fecal pellets contributed a substantial flux during short periods in late summer in the Ross Sea (6–21% of the total carbon flux using conservative estimates of fecal pellet carbon contents; Smith et al., 2011b), but in most periods flux appeared to be dominated by marine snow and phytodetritus. This pattern is not necessarily characteristic of all Antarctic waters; Laurenceau-Cornec et al. (2015) found that in the Kergulen Plateau vertical flux was dominated by fecal material, especially when expressed on a carbon basis (only 30% of the carbon flux was contributed by phytodetritus). Similarly, Ducklow et al. (2015) found that phytodetritus from *Phaeocystis anatarctica* in the Amundsen Polynya dominated the vertical flux, although fecal pellets contributed up to 40% of the flux during short episodes. The differences among these studies suggest the need to accurately identify the controls on carbon export efficiency, which appear to include small spatio-temporal variations in ecosystem structure and the components and interactions within the plankton.

Nepheloid layers were frequently found in this study, particularly in late summer, and influenced waters within 100 m of the sediments (**Figures 3, 4a, b**). The material within the nepheloid layer at times included pigmented matter (**Figure 4**), suggesting that this carbon pool had entered the bottom layer recently (within the growing season), given the expectation that labile POC would be remineralized relatively rapidly in the sediments

(DiTullio et al., 2000). However, Mincks et al. (2005) reported the half-life of labile sedimentary POC off the West Antarctic Peninsula to be on the order of 6 months. If also true in the Ross Sea, some of the pigmented POC we observed might have been derived from the previous year. Regardless, the presence of pigmented organics suggests that a fraction of the resuspended material is labile and could be used by benthic fauna. Aggregate numbers also increased in the nepheloid layer. This enhancement could result from in situ formation within the turbulent bottom layer or simply the resuspension of aggregates within the nepheloid layer. Given that aggregates appear to be actively remineralized within the water column (based on their exponential disappearance), aggregates within the nepheloid layer likely represent those that sank rapidly and were oxidized minimally during their vertical transit.

Ghost colonies appeared to be remineralized very rapidly (**Figure 8**); indeed, numbers were reduced by 90% in the top 120 m of our observations, with only 1% of surface numbers remaining below 320 m. As such, ghost colonies do not likely represent a significant flux of carbon to the sediments (in this area at a depth of ~650 m), consistent with the analysis of Wassmann et al. (2006) for bulk POC generated by *Phaeocystis globosa*. However, we emphasize that rapidly sinking particles, though they do not contribute substantially to standing stocks, can be important in vertical flux, so that the role of ghost colonies in export remains uncertain. When the POC mean distribution in late summer in Year 4 (**Figure 4**) is compared to that of ghost colonies, we find that bulk POC appears to be remineralized slightly more slowly than ghost colonies. Specifically, 25% of the surface POC remains at 500 m, whereas less than 1% of ghost colony POC remains at that depth. It is possible that ghost colonies are transformed quickly and sink rapidly from the water column, and hence are not observed at depth by our camera system, but there are no data to adequately test this hypothesis.

5. Conclusions

Aggregates constitute an important component of the biological carbon cycle in the Ross Sea. Despite the large uncertainties in estimating the absolute carbon concentrations in aggregates relative to other potential contributors (e.g., ghost colonies, fecal pellets), they contribute significantly to the total sub-euphotic zone POC and are likely the dominant mode of organic carbon vertical transport in the Ross Sea in early and late summer. Variations in aggregate abundance through time are significant, but late summer appears to be the season when aggregate abundance is maximal, coincident with the period of maximum vertical mass export from the surface layers (Smith et al., 2011b). Hence the formation of aggregates and the period of maximum surface production are temporally decoupled. While different forms of discrete aggregates were observed (such as *Phaeocystis* ghost colonies), loosely associated aggregates appeared to make the largest contribution to total aggregate abundance. The dominant aggregate size class was the smallest one measured, and size distributions were consistent in both seasons and with depth. Nepheloid layers occurred in late summer, and aggregate abundance was elevated within them.

Although we estimated that the contribution of aggregates to the total particulate organic carbon pool was ca. 20% over the entire water column, these estimates have substantial uncertainties associated with them due to the assumptions made to estimate aggregate POC. Those assumptions, the unknown and variable sinking rates of aggregates, and the uncertainties in the structure and role of aggregates in the Ross Sea and Southern Ocean, suggest that further efforts are needed to constraint their role in biogeochemical cycles of the Antarctic. Such efforts need new approaches to quantifying the abundance and carbon contributions of aggregates to reduce the quantitative uncertainties of their role in the biological pump.

Data Accessibility Statement

All aggregate data are archived and publically available at the BCO-DMO website (http://www.bco-dmo.org/dataset/719478; https://www.bco-dmo.org/dataset/768570).

Acknowledgements

We thank J Peloquin, A Shields, J Dreyer, H Ballenger, and all the IVARS workers for assistance in the field, and D McGillicuddy for providing the images used in Figure 7. J Blancher provided computational assistance. The help of the crew and officers of *the RVIB N Palmer*, the *USCGC Polar Star* and the *USCGC Polar Sea* was essential.

Funding information

This research was supported by the National Science Foundation (OPP-0087401). This is VIMS contribution number 3831.

Competing interests

The authors have no competing interests to declare.

Author contributions

- Contributed to conception and design: VA, WS
- Contributed to acquisition of data: VA, WS
- Contributed to analysis and interpretation of data: VA, WS
- Drafted and revised the article: VA, WS

References

Alldredge, AL. 1998. The carbon, nitrogen and mass content of marine snow as a function of aggregate size. *Deep-Sea Res I* **45**: 529–542. DOI: https://doi.org/10.1016/S0967-0637(97)00048-4

Alldredge, AL and **Gotschalk, CC.** 1989. Direct observations of the mass flocculation of diatom blooms: characteristics, settling velocities and formation of diatom aggregates. *Deep-Sea Res* **36**: 159–171. DOI: https://doi.org/10.1016/0198-0149(89)90131-3

Arrigo, KR, Robinson, DH, Worthen, DL, Dunbar, RB, DiTullio, GR, van Woert, M and **Lizotte, MP.** 1999. Phytoplankton community structure and the drawdown of nutrients and CO_2 in the Southern

Ocean. *Science* **283**: 365–367. DOI: https://doi.org/10.1126/science.283.5400.365

Arrigo, KR, van Dijken, G and **Long, M.** 2008. Coastal Southern Ocean: a strong anthropogenic CO_2 sink. *Geophys Res Lett* **35**: L21602. DOI: https://doi.org/10.1029/2008GL035624

Asper, V and **Smith, WO, Jr.** 1999. Particle fluxes during austral spring and summer in the southern Ross Sea (Antarctica). *J Geophys Res* **104**: 5345–5359. DOI: https://doi.org/10.1029/1998JC900067

Asper, V and **Smith, WO, Jr.** 2003. Abundance, distribution and sinking rates of aggregates in the Ross Sea Polynya. *Deep-Sea Res I* **50**: 131–150. DOI: https://doi.org/10.1016/S0967-0637(02)00146-2

Bach, LT, Boxhammer, T, Larsen, A, Hildebrandt, N, Schulz, KG and **Riebesell, U.** 2016. Influence of plankton community structure on the sinking velocity of marine aggregates. *Global Biogeochem Cy* **30**: 1145–1165. DOI: https://doi.org/10.1002/2016GB005372

Bishop, JKB, Wood, TJ, Davis, RE and **Sherman, JT.** 2004. Robotic observations of enhanced carbon biomass and export at 55°S during SOFeX. *Science* **304**: 417–420. DOI: https://doi.org/10.1126/science.1087717

Burd, AB and **Jackson, GA.** 2009. Particle aggregation. *Annu Rev Mar Sci* **1**: 65–90. DOI: https://doi.org/10.1146/annurev.marine.010908.163904

Caron, DA, Dennett, MR, Lonsdale, DJ, Moran, DM and **Shalapyonok, L.** 2000. Microzooplankton herbivory in the Ross Sea, Antarctica. *Deep-Sea Res II* **47**: 3249–3272. DOI: https://doi.org/10.1016/S0967-0645(00)00067-9

Cavagna, A-J, Dehairs, F, Bouillon, S, Woule-Ebongué, V, Planchon, F, Delille, B and **Bouloubassi, I.** 2013. Water column distribution and carbon isotopic signal of cholesterol, brassicasterol and particulate organic carbon in the Atlantic sector of the Southern Ocean. *Biogeosciences* **10**: 2787–2801. DOI: https://doi.org/10.5194/bg-10-2787-2013

De La Rocha, C and **Passow, U.** 2007. Factors influencing the sinking of POC and the efficiency of the biological carbon pump. *Deep-Sea Res II* **54**: 639–658. DOI: https://doi.org/10.1016/j.dsr2.2007.01.004

DiTullio, GR, Grebmeier, JM, Arrigo, KR, Lizotte, MP, Robinson, DH, Leventer, A, Barry, JP, van Woert, ML and **Dunbar, RB.** 2000. Rapid and early export of *Phaeocystis antarctica* blooms in the Ross Sea Antarctica. *Nature* **404**: 595–598. DOI: https://doi.org/10.1038/35007061

Ducklow, HW, Wilson, SE, Post, AF, Stammerjohn, SE, Erickson, M, Lee, S, Lowry, KE, Sherrell, RM and **Yager, PL.** 2015. Particle flux on the continental shelf in the Amundsen Sea Polynya and Western Antarctic Peninsula. *Elem Sci Anth*, 3–46. DOI: https://doi.org/10.12952/journal.elementa.000046

Ebersbach, F and **Trull, TW.** 2008. Sinking particle properties from polyacrylamide gels during the KErguelen Ocean and Plateau compared study (KEOPS): Zooplankton control of carbon export in an area of persistent natural iron inputs in the Southern Ocean. *Limnol Oceanogr* **53**: 212–224. DOI: https://doi.org/10.4319/lo.2008.53.1.0212

Gardner, WD, Richardson, MJ and **Smith, WO, Jr.** 2000. Seasonal build-up and loss of POC in the Ross Sea. *Deep-Sea Res II* **47**: 3423–3450. DOI: https://doi.org/10.1016/S0967-0645(00)00074-6

Gowing, MM, Garrison, DL, Kunze, HB and **Winchell, CJ.** 2001. Biological components of Ross Sea short-term particle fluxes in the austral summer of 1995–1996. *Deep-Sea Res I* **48**: 2645–2671. DOI: https://doi.org/10.1016/S0967-0637(01)00034-6

Guidi, L, Stemmann, L, Jackson, GA, Ibanez, F, Claustre, H, Legendre, L, Picheral, M and **Gorskya, G.** 2009. Effects of phytoplankton community on production, size, and export of large aggregates: a world-ocean analysis. *Limnol Oceanogr* **54**: 1951–1963. DOI: https://doi.org/10.4319/lo.2009.54.6.1951

Honjo, S, Doherty, KW, Agrawal, YC and **Asper, VL.** 1984. Direct optical assessment of large amorphous aggregates (marine snow) in the deep ocean. *Deep-Sea Res* **31**: 67–76. DOI: https://doi.org/10.1016/0198-0149(84)90073-6

Iversen, MH and **Ploug, H.** 2013. Temperature effects on carbon-specific respiration rate and sinking velocity of diatom aggregates – potential implications for deep ocean export processes. *Biogeosciences* **10**: 4073–4085. DOI: https://doi.org/10.5194/bg-10-4073-2013

Jackson, GA. 1990. A model of the formation of marine algal flocs by physical coagulation processes. *Deep-Sea Res* **37**: 1197–1211. DOI: https://doi.org/10.1016/0198-0149(90)90038-W

Jackson, GA, Waite, AM and **Boyd, PW.** 2005. Role of algal aggregation in vertical carbon export during SOIREE and in other low biomass environments. *Geophys Res Lett* **32**: L13607. DOI: https://doi.org/10.1029/2005GL023180

Jones, RM and **Smith, WO, Jr.** 2017. The influence of short-term events on the hydrographic and biological structure of the southwestern Ross Sea. *J Mar Systems* **166**: 184–195. DOI: https://doi.org/10.1016/j.jmarsys.2016.09.006

Kaufman, DE, Friedrichs, MAM, Smith, WO, Jr., Queste, BY and **Heywood, KJ.** 2014. Biogeochemical variability in the southern Ross Sea as observed by a glider deployment. *Deep-Sea Res I* **92**: 93–106. DOI: https://doi.org/10.1016/j.dsr.2014.06.011

Kiørboe, T and **Hansen, JLS.** 1993. Phytoplankton aggregate formation: observations of patterns and mechanisms of cell sticking and the significance of exopolymeric material. *J Plankton Res* **9**: 993–1018. DOI: https://doi.org/10.1093/plankt/15.9.993

Lam, PJ and **Bishop, JKB.** 2007. High biomass low export regimes in the Southern Ocean. *Deep-Sea Res II* **54**: 601–638. DOI: https://doi.org/10.1016/j.dsr2.2007.01.013

Lampitt, RS, Hillier, WR and **Challenor, PG.** 1993. Seasonal and diel variations in the open

ocean concentration of marine snow aggregates. *Nature* **362**: 737–739. DOI: https://doi.org/10.1038/362737a0

Lancelot, C, Keller, MD, Rousseau, V, Smith, WO, Jr. and **Mathot, S.** 1998. Autecology of the marine haptophyte *Phaeocystis* sp. In: Anderson, DM, Cembella, AD and Hallegraeff, GM (eds.), *Physiological Ecology of Harmful Algal Blooms*, NATO ASI Series, Vol G41, pp. 211–244. Heidelberg: Springer-Verlag.

Laurenceau-Cornec, EC, Trull, TW, Davies, DM, Bray, SG, Doran, J, Planchon, F, Carlotti, F, Jouandet, MP, Cavagna, AJ, Waite, AM and **Blain, S.** 2015. The relative importance of phytoplankton aggregates and zooplankton fecal pellets to carbon export: insights from free-drifting sediment trap deployments in naturally iron-fertilised waters near the Kerguelen Plateau. *Biogeosciences* **12**: 1007–1027. DOI: https://doi.org/10.5194/bg-12-1007-2015

Mathot, S, Smith, WO, Jr., Carlson, CA and **Garrison, DL.** 2000. Estimate of *Phaeocystis* sp. carbon biomass: methodological problems related to the mucilaginous nature of the colonial matrix. *J Phycol* **36**: 1049–1056. DOI: https://doi.org/10.1046/j.1529-8817.2000.99078.x

Mincks, SL, Smith, CR and **DeMaster, DJ.** 2005. Persistence of labile organic matter and microbial biomass in Antarctic shelf sediments: evidence of a sediment 'food bank'. *Mar Ecol Prog Ser* **300**: 3–19. DOI: https://doi.org/10.3354/meps300003

Mosby, AF and **Smith, WO, Jr.** 2015. Phytoplankton growth rates in the Ross Sea, Antarctica. *Aquat Microb Ecol* **74**: 157–171. DOI: https://doi.org/10.3354/ame01733

Passow, U, Alldredge, AL and **Logan, BE.** 1994. The role of particulate carbohydrate exudates in the flocculation of diatom blooms. *Deep-Sea Res I* **41**: 335–357. DOI: https://doi.org/10.1016/0967-0637(94)90007-8

Reigstad, M and **Wassmann, P.** 2007. Does *Phaeocystis* spp. contribute significantly to vertical export of organic carbon? *Biogeochemistry* **83**: 217–234. DOI: https://doi.org/10.1007/978-1-4020-6214-8_16

Riebesell, U. 1993. Aggregation of *Phaeocystis* during phytoplankton spring blooms in the southern North *Sea. Mar Ecol Prog Ser* **96**: 281–289. DOI: https://doi.org/10.3354/meps096281

Schoemann, V, Becquevort, S, Stefels, J, Rousseau, V and **Lancelot, C.** 2005. *Phaeocystis* blooms in the global ocean and their controlling mechanisms: a review. *J Sea Res* **53**: 43–66. DOI: https://doi.org/10.1016/j.seares.2004.01.008

Sedwick, PN, Marsay, CM, Sohst, BM, Aguilar-Islas, AM, Lohan, MC, Long, MC, Arrigo, KR, Dunbar, RB, Saito, MA, Smith, WO, Jr. and **DiTullio, GR.** 2011. Early season depletion of dissolved iron in the Ross Sea polynya: implications for iron dynamics on the Antarctic continental shelf. *J Geophys Res* **116**: C12019. DOI: https://doi.org/10.1029/2010JC006553

Smith, WO, Jr., Ainley, DG, Arrigo, KR and **Dinniman, MS.** 2014. The oceanography and ecology of the Ross Sea. *Annu Rev Mar Sci* **6**: 469–487. DOI: https://doi.org/10.1146/annurev-marine-010213-135114

Smith, WO, Jr. and **Asper, VA.** 2001. The influence of phytoplankton assemblage composition on biogeochemical characteristics and cycles in the southern Ross Sea, Antarctica. *Deep-Sea Res I* **48**: 137–161. DOI: https://doi.org/10.1016/S0967-0637(00)00045-5

Smith, WO, Jr., Asper, V, Tozzi, S, Liu, X and **Stammerjohn, SE.** 2011a. Continuous fluorescence measurements in the Ross Sea, Antarctica: scales of variability. *Progr Oceanogr* **88**: 28–45. DOI: https://doi.org/10.1016/j.pocean.2010.08.002

Smith, WO, Jr. and **Kaufman, DE.** 2018. Climatological temporal and spatial distributions of nutrients and particulate matter in the Ross Sea. *Progr Oceanogr* **168**: 182–195. DOI: https://doi.org/10.1016/j.pocean.2018.10.003

Smith, WO, Jr., Marra, J, Hiscock, MR and **Barber, RT.** 2000. The seasonal cycle of phytoplankton biomass and primary productivity in the Ross Sea, Antarctica. *Deep-Sea Res I* **47**: 3119–3140. DOI: https://doi.org/10.1016/S0967-0645(00)00061-8

Smith, WO, Jr., McGillicuddy, DJ, Jr., Olson, EB, Kosnyrev, V, Peacock, EE and **Sosik, HM.** 2017. Mesoscale variability in intact and ghost colonies of *Phaeocystis antarctica* in the Ross Sea: distribution and abundance. *J Mar Systems* **166**: 97–107. DOI: https://doi.org/10.1016/j.jmarsys.2016.05.007

Smith, WO, Jr. and **Nelson, DM.** 1985. Phytoplankton bloom produced by a receding ice edge in the Ross Sea: Spatial coherence with the density field. *Science* **227**: 163–166. DOI: https://doi.org/10.1126/science.227.4683.163

Smith, WO, Jr., Nelson, DM, DiTullio, GR and **Leventer, AR.** 1996. Temporal and spatial patterns in the Ross Sea: phytoplankton biomass, elemental composition, productivity and growth rates. *J Geophys Res* 101: 18,455–18,466. DOI: https://doi.org/10.1029/96JC01304

Smith, WO, Jr., Shields, AR, Dreyer, JC, Peloquin, JA and **Asper, V.** 2011b. Interannual variability in vertical export in the Ross Sea: magnitude, composition, and environmental correlates. *Deep-Sea Res I* **58**: 147–159. DOI: https://doi.org/10.1016/j.dsr.2010.11.007

Smith, WO, Jr., Shields, AR, Peloquin, JA, Catalano, G, Tozzi, S, Dinniman, MS and **Asper, VA.** 2006. Interannual variations in nutrients, net community production, and biogeochemical cycles in the Ross Sea. *Deep-Sea Res II* **53**: 815–833. DOI: https://doi.org/10.1016/j.dsr2.2006.02.014

Smith, WO, Jr., Tozzi, S, Sedwick, PW, DiTullio, GR, Peloquin, JA, Long, M, Dunbar, R, Hutchins, DA and **Kolber, Z.** 2013. Spatial and temporal variations in variable fluorescence in the Ross Sea (Antarctica): environmental and biological correlates. *Deep-Sea Res I* **79**: 141–155. DOI: https://doi.org/10.1016/j.dsr.2013.05.002

Sweeney, C, Hansell, DA, Millero, FD, Takahashi, T, Gordon, LI, Carlson, CA, Codispoti, LA, Smith, WO,

Jr. and **Marra, J.** 2000. Biogeochemical regimes, net community production and carbon export in the Ross Sea, Antarctica. *Deep-Sea Res II* **47**: 3369–3394. DOI: https://doi.org/10.1016/S0967-0645(00)00072-2

Tagliabue, A and **Arrigo, KR.** 2003. Anomalously low zooplankton abundance in the Ross Sea: an alternative explanation. *Limnol Oceanogr* **48**: 686–699. DOI: https://doi.org/10.4319/lo.2003.48.2.0686

Thomson, RE and **Fine, IV.** 2003. Estimating mixed layer depth from oceanic profile data. *J Atmos Ocean Tech* **20**: 319–329. DOI: https://doi.org/10.1175/1520-0426(2003)020<0319:EMLDFO>2.0.CO;2

Turner, JT. 2002. Zooplankton fecal pellets, marine snow and sinking phytoplankton blooms, *Aquat Microb Ecol* **27**: 57–102. DOI: https://doi.org/10.3354/ame027057

Wassmann, P, Reigstad, M, Haug, T, Rudels, B, Carroll, ML, Hop, H, Gabrielsen, GW, Falk-Petersen, S, Denisenko, SG, Arashkevich, E, Slagstad, D and **Pavlova, O.** 2006. Food webs and carbon flux in the Barents Sea. *Progr Oceanogr* **71**: 232–287. DOI: https://doi.org/10.1016/j.pocean.2006.10.003

Wassmann, P, Vernet, M, Mitchell, BG and **Rey, F.** 1990. Mass sedimentation of *Phaeocystis pouchetii* in the Barents Sea. *Mar Ecol Prog Ser* **66**: 183–195. DOI: https://doi.org/10.3354/meps066183

Wassmann, P, Ypma, JE and **Tselepides, A.** 2000. Vertical flux of faecal pellets and microplankton on the shelf of the oligotrophic Cretan Sea (NE Mediterranean Sea). *Progr Oceanogr* **46**: 241–258. DOI: https://doi.org/10.1016/S0079-6611(00)00021-5

How to cite this article: Asper, VL and Smith, WO. 2019. Variations in the abundance and distribution of aggregates in the Ross Sea, Antarctica. *Elem Sci Anth,* 7: 23. DOI: https://doi.org/10.1525/elementa.355

Domain Editor-in-Chief: Jody W. Deming, School of Oceanography, University of Washington, US

Associate Editor: Kevin Arrigo, Environmental Earth System Science, Stanford University, US

Knowledge Domain: Ocean Science

Submitted: 30 October 2018 **Accepted:** 15 April 2019 **Published:** 07 June 2019

ELEMENTA Science of the Anthropocene

Elem Sci Anth is a peer-reviewed open access journal published by University of California Press.

OPEN ACCESS